DOI: 10.1002/ejic.200500222

Polymorphism Driven by π–π Stacking and van der Waals Interactions: Preparation and Characterization of Polymorphic Vanadium Crystals of $[V^{V}O(Hacshz)(OEt)]$ and $[V^{IV}(Hacshz)_2]$

Yinshi Jin[a] and Myoung Soo Lah*[a]

Keywords: Crystal engineering / Pi interactions / Polymorphism / Supramolecular chemistry / Vanadium

Polymorphic mono-oxo mono-alkoxo square-pyramidal $[V^{V}O(Hacshz)(OEt)]$ (where $Hacshz^{2-}$ is a doubly deprotonated dianionic acetylacetosalicylhydrazone; thick plate-shaped dark-greenish-brown crystals for **1a** and block-shaped dark-reddish-brown crystals for **1b**) and mononuclear trigonal-prismatic $[V^{IV}(Hacshz)_2]$ (block-shaped dark-bluish-brown crystals for **2a** and triangular-shaped dark-violet crystals for **2b**) were synthesized and characterized. The crystals were prepared by simple addition of vanadium(III) acetylacetonate to an ethanol solution of salicylhydrazide (H_3shz). Depending on the ratio of the ligand to the metal ion, the extent of exposure to molecular oxygen, and the filtration of the intermediate, various polymorphs could be obtained as both mixtures and pure forms. A common π–π stacked dimeric species was observed in both polymorphs **1a** and **1b**. The dimeric species behaves as a common repeating motif, but in different interaction modes. A second type of π–π interaction, in addition to van der Waals interactions, was observed in crystals of **1a**, while only van der Waals interactions were observed in crystal **1b**. Another type of π–π-stacked dimeric vanadium(IV) species again behaves as a repeating motif in crystals of **2a** and **2b**, but in different interaction modes. The thermal properties, such as the decomposition behavior and melting points, of the two different polymorphs of the same vanadium complexes are very similar but not identical.

Introduction

Crystal engineering and supramolecular chemistry are the planning and construction of the structure and properties of materials using relatively weak interactions such as hydrogen bonding,[1] van der Waals interactions,[2] dipole interactions,[3] π–π stacking interactions,[4] and coordination[5] by appropriate design of the molecular building units. Understanding these weak intermolecular interactions is important to comprehend the factors governing crystal engineering and supramolecular chemistry. The building units are arranged into crystalline materials or supramolecular entities as a result of the accumulation of several weak intermolecular interactions. Relatively strong and directional hydrogen-bonding interactions and partly directional π–π stacking interactions are most commonly utilized for rational design in crystal engineering and supramolecular chemistry.[6] Nondirectional van der Waals and dipole interactions are also used to orient molecules in crystals or in solution.[7] It is usually very difficult to utilize these weak intermolecular interactions in rational design because these different types of interactions act together in a concerted rather than in a separate way, so the prediction of the desired structure is often impossible.

Polymorphism − the different packing arrays of the same building units − is frequently found in crystalline materials of some organic and inorganic complexes.[8] This phenomenon is of interest because it utilizes the different intermolecular interactions of the same structural entity for the formation of different polymorphs and, therefore, understanding their role in polymorphism can be utilized for molecular and/or crystal design. There are many examples of polymorphs involving hydrogen-bonding interactions together with other weak interactions.[9] However, only a few examples are known where π–π stacking interactions without hydrogen-bonding interactions play the major role in the formation of different polymorphic crystals.[10] π–π Stacking interactions have been recognized in solid state and supramolecular design, and have been utilized in many research areas such as molecular conductors,[11] molecular machines,[12] and electronics.[13]

Recently, we reported the synthesis and characterization of the mono-oxo mono-alkoxo square-pyramidal vanadium(V) complex $[VO(Hacshz)(OEt)]$.[14] During our investigation of this complex, we identified a polymorphism phenomenon where the building unit is arranged in different packing interaction modes. In addition, we isolated $[V^{IV}(Hacshz)_2]$ as an intermediate or side product, which also appeared in two different packing modes. In both com-

[a] Department of Chemistry and Applied Chemistry, College of Science and Technology, Hanyang University,
1271 Sa-1-dong, Ansan, Kyunggi-do 426-791, Korea
Fax: +82-31-407-3863
E-mail: mslah@hanyang.ac.kr

plexes, the intermolecular interactions involved are only π–π stacking and van der Waals interactions, with no hydrogen-bonding interactions. Thus, these complexes could serve as simplified model systems in which the complexity of combined interactions is reduced to only two kinds in polymorphic crystal packing. Here, we report the synthesis and characterization of the polymorphic mono-oxo monoalkoxo square-pyramidal vanadium(v) complex [VO(Hacshz)(OEt)] (**1**) and the mononuclear trigonal-prismatic vanadium(iv) complex [V(Hacshz)$_2$] (**2**). Various π–π stacking interaction modes of the same motif, acetylacetosalicylhydrazone, are presented and discussed.

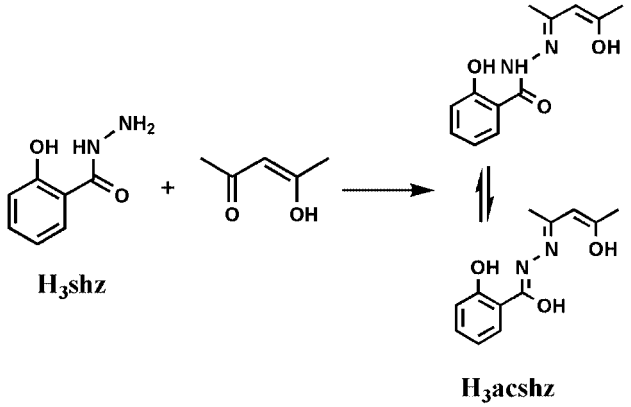

Scheme 1.

Results and Discussion

Preparation and Characterization of Polymorphic Vanadium Crystals

The vanadium(v) complex [V^{V}O(Hacshz)(OEt)] (**1**) was prepared following a reported method.[14] The complex was synthesized by simple addition of one equivalent of vanadium(iii) acetylacetonate to an ethanol solution of H_3shz in a beaker in air; Hacshz^{2-} was formed by the Schiff-base condensation reaction of H_3shz with acetylacetonate in situ (Scheme 1). In repeated experiments under exactly the same conditions, we noticed that the products were a mixture of two slightly different shaped and colored crystals, namely thick, plate-shaped, dark-greenish-brown crystals (**1a**) and block-shaped, dark-reddish-brown crystals (**1b**; Scheme 2). The IR spectrum of **1a** is very similar to that of **1b**, but not identical. The characteristic V=O stretching band is observed at 998 cm^{-1} for **1a** but at 1001 cm^{-1} for **1b**. The crystals also have different physical properties: **1a** melts in the range 115.1–116.9 °C while **1b** melts over a slightly higher temperature range (117.2–118.8 °C). Complexes **1a** and **1b** are indistinguishable in solution, as expected. The ^{1}H NMR spectrum of **1a** in chloroform is identical to that of **1b**.

When the reaction was performed under the same conditions but in a closed 30-mL vial, a crystalline precipitate of **2** formed within a day. Complex **2** was filtered off, and, on standing, the filtrate produced only crystals of **1a**. Complex **2** was confirmed to be [V^{IV}(Hacshz)$_2$], which has no oxo group and two dianionic Hacshz^{2-} ligands per vanadium(iv) ion. In the presence of limited amounts of oxygen, the vanadium(iii) ion is oxidized to the vanadium(iv) complex. Complex **1a** could also be obtained as the sole product with a 2:1 ratio of H_3shz and vanadium(iii) acetylacetonate in ethanol solution in the presence of enough oxygen. Surprisingly, **1b** was obtained as the sole product with a 3:1 ratio of H_3shz and vanadium(iii) acetylacetonate, while a mixture of **1a** and **1b** was obtained with a 1:1 ratio of H_3shz and vanadium(iii) acetylacetonate. It is not clear why different polymorphs are obtained with different amounts of metal ions.

The mononuclear vanadium(iv) complex **2** was obtained when the amount of oxygen was limited. Careful examination of the crystalline precipitate **2** revealed two types of crystalline material, namely block-shaped, dark-bluish-brown crystals (**2a**) as a major species and triangular-

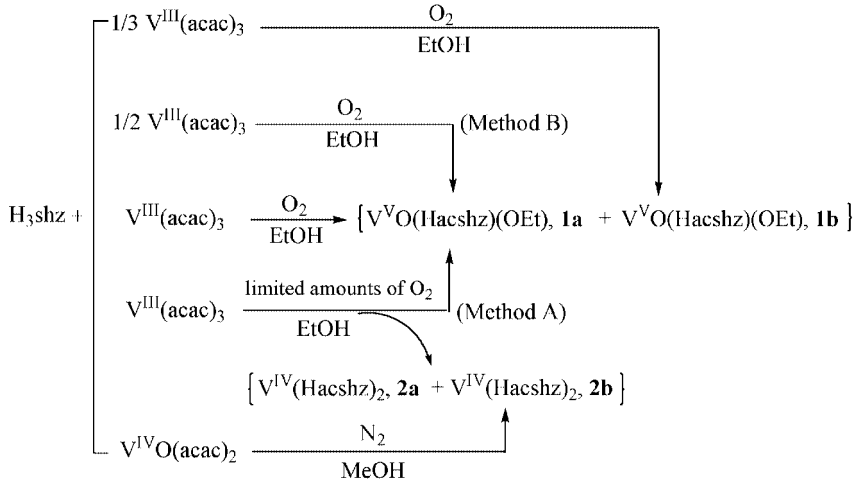

Scheme 2.

shaped, dark-violet crystals (**2b**) as a very minor species. Complex **2b** is identical to the previously reported crystal structure of $[V^{IV}(Hacshz)_2,]$, which was prepared from H_3shz and vanadyl(IV) acetylacetonate in methanol under nitrogen.[16] Magnetic susceptibility measurements of **2a** (μ_{eff} = 1.80 μ_B after a diamagnetic correction with Pascal's constants) suggest that the complex contains a paramagnetic d^1 vanadium(IV) ion.

Crystal Structure of $[V^{V}O(Hacshz)(OEt)]$ (1)

The molecular structure of **1a** is very similar to that of the previously reported square-pyramidal dialkoxo-bound monooxo-vanadium(V) complex **1b** (Table 1).[14] An ORTEP drawing of **1a** is shown in Figure 1. $Hacshz^{2-}$ serves as a tridentate ligand to form five- and six-membered chelating rings. An ethoxide anion occupies the remaining basal site of the square-pyramidal oxovanadium(V) center.

Table 1. Bond lengths [Å] and bond angles [°] for **1a** and **1b**.

	1a	1b		1a	1b
V1–O1	1.589(1)	1.582(1)	V1–O4	1.863(1)	1.862(1)
V1–O3	1.930(1)	1.939(1)	V1–N2	2.073(1)	2.096(1)
V1–O5	1.766(1)	1.749(1)			
O1–V1–O3	105.67(5)	101.08(6)	O1–V1–O4	103.66(5)	102.90(6)
O1–V1–O5	106.78(6)	106.68(6)	O1–V1–N2	99.92(5)	100.66(6)
O4–V1–O3	146.35(5)	150.10(5)	O5–V1–O3	87.67(5)	90.63(5)
O3–V1–N2	74.97(4)	74.81(5)	O5–V1–O4	99.36(5)	99.28(5)
O4–V1–N2	84.10(5)	83.39(5)	O5–V1–N2	151.30(5)	151.08(6)

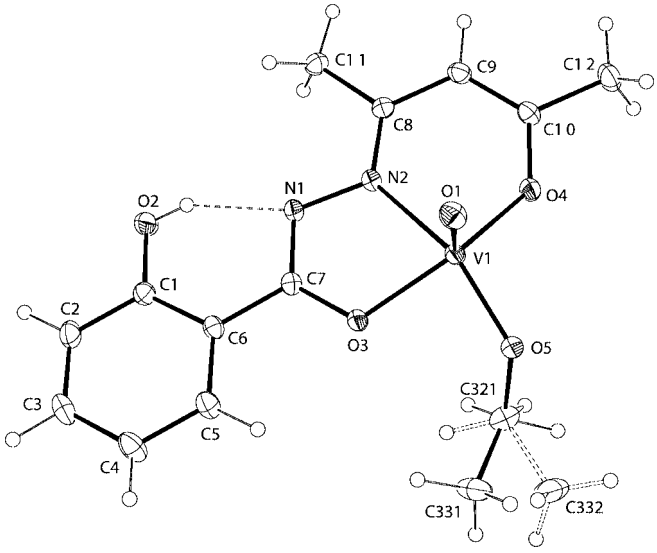

Figure 1. ORTEP drawing of complex **1a**. The minor part of the disordered ethoxide is represented by broken lines.

The packing of **1a** (Figure 2, a) is quite different from that of **1b** (Figure 3, a). In **1b**, the π–π stacked dimeric species (Figure 3, parts a and b) interact only through van der Waals interactions to form a three-dimensional crystal

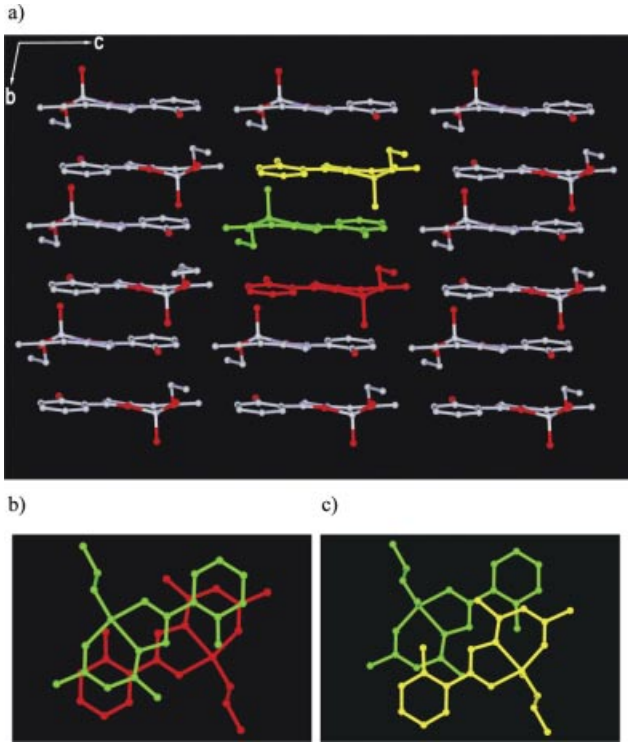

Figure 2. (a) Packing of **la**. The alternation of two types of π–π stacking interactions forms a one-dimensional chain. Only van der Waals interactions are observed between the π–π stacked one-dimensional chains. (b) Type I: the π–π stacking interaction is between the phenoxy and acetylacetohydrazone groups. (c) Type II: the π–π stacking interaction is similar to that of type I but slightly displaced.

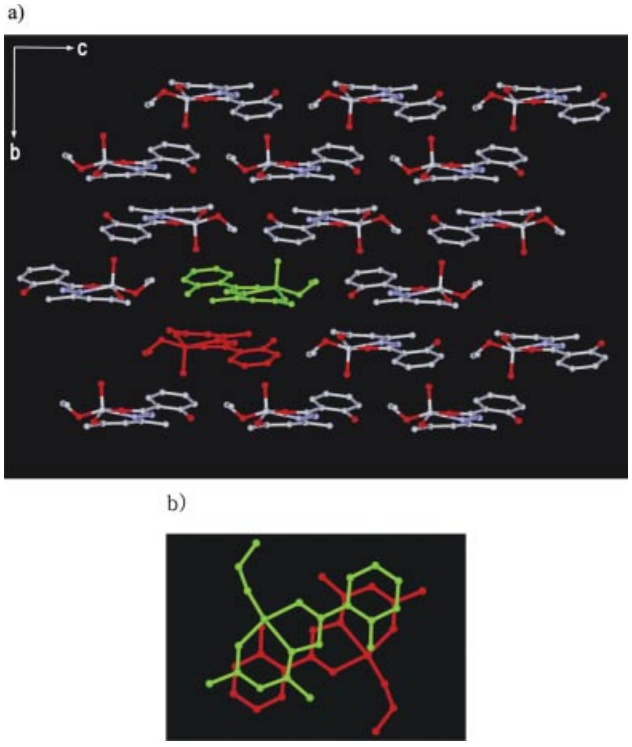

Figure 3. (a) Packing of **lb**. The three-dimensional structure is formed by van der Waals interactions between the π–π stacked dimeric species. (b) Type-I π–π stacking interaction.

Table 2. π–π stacking interaction distances [Å] for **1a**, **1b**, **2a**, and **2b**.

Type I			Type II			
	1a	**1b**		**1a**		
N1···C7	3.368(2)	3.300(2)	C1···C9	3.442(2)		
C6···C10	3.305(3)	3.315(3)	C7···C11	3.453(2)		
C2···C8	3.421(2)	3.350(2)				
V1···O2	3.418(2)	3.190(2)				
Type III			Type IV		Type V	
	2a	**2b**		**2a**		**2b**
C1b···C7b	3.557(5)	3.655(3)	C2a···C7a	3.478(5)	N1a···C10a	3.303(2)
C2b···C2b	3.511(5)	3.495(3)	C5a···C8a	3.624(5)	C1a···C12a	3.655(3)

structure. A π–π stacking interaction (type I) between the phenoxy group and the conjugated acetylacetohydrazones [N1···C7 = 3.300(2), C6···C10 = 3.315(3), C2···C8 = 3.350(2) Å] is observed in the dimeric species (part b in Figure 3 and Table 2). An additional close contact between the vanadium atom and the symmetry-related O2 atom [3.190(2) Å] is also observed.

In **1a**, two different types of π–π stacking interactions are seen. The first type of π–π stacking interaction (type I) is the same as that found in **1b** (parts b in Figure 2 and Figure 3, and Table 2). The only difference in both dimeric species is in the conformation of the ethoxide groups. The dimeric species in crystal **1a** interacts with two neighboring dimeric species to form a one-dimensional chain through a second type of π–π stacking interaction (type II). The type II interaction is similar to that of type I, but slightly displaced (part c in Figure 2 and Table 2). The type II stacking interaction [C1···C9 = 3.442(2), C7···C11 = 3.453(2) Å] is longer than the type I interaction. In **1a**, the one-dimensional chains connect by alternating the two types of π–π stacking interactions to form a three-dimensional crystal structure containing van der Waals interactions (Figure 2, a).

Crystal Structure of $[V^{IV}(Hacshz)_2]$ (2)

The molecular structure of **2a** is also very similar to that of **2b**. As in **2b**, **2a** has a trigonal-prismatic coordination sphere with pseudo-C_3 symmetry (Figure 4 and Table 3). The bite distances of the prismatic edges formed by the two five-membered chelating bidentate ligands are 2.417(3) Å for O3a···N2a and 2.406(3) Å for O3b···N2b; the bite angles are 75.3(1)° for O3a–V1–N2a and 74.6(1)° for O3b–V1–N2b. The length of the remaining prismatic edge formed by the two alkoxo atoms (O4a···O4b) is 2.505(2) Å, and the O4a–V1–O4b angle is 80.8(1)°. The twist angles[17] determined by the relative orientation of two opposite triangular faces are 4.3° for **2a** and 4.6° for **2b**.

Even though the molecular structure of **2a** is very similar to that of **2b**, the packing of **2a** is quite different to that of **2b**. In **2a**, two different types of π–π stacking interactions (types III & IV) are observed, as in the crystal structure of **1a**. The third type of π–π stacking interaction (type III) is seen between the salicylhydrazones [C2b···C2b = 3.511(5), C1b···C7b = 3.557(5) Å; part b in Figure 5 and Table 2]. As

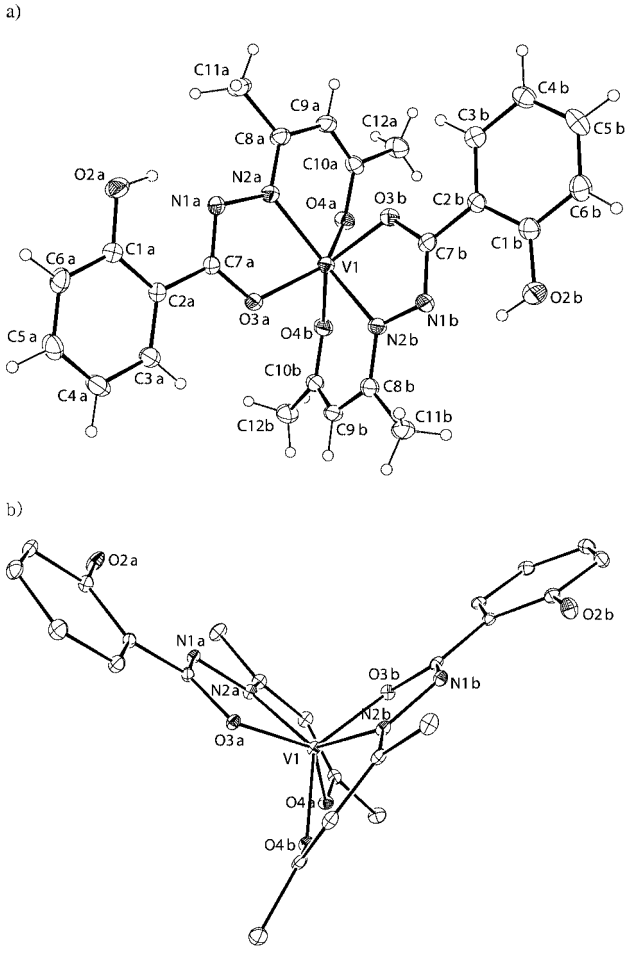

Figure 4. (a) ORTEP drawing of complex **2a** with numbering Scheme. (b) View showing the pseudo-C_3-symmetric trigonal-prismatic coordination geometry of the vanadium center.

in **1a**, the π–π stacked dimeric species formed interacts with two neighboring dimeric species to form a one-dimensional chain through the fourth type of π–π stacking interaction (type IV). The type IV interaction is again longer than the type III interaction [C2a···C7a = 3.478(5), C5a···C8a = 3.624(5) Å; Figure 5 (c) and Table 2]. The one-dimensional chains connect through two types of π–π stacking interactions to form a three-dimensional structure containing van der Waals interactions.

Table 3. Bond lengths [Å], bond angles [°], bite distances [Å], and bite angles [°] for **2a** and **2b**.

	2a	**2b**		**2a**	**2b**
V1–O3a	1.928(2)	1.931(1)	V1–O3b	1.918(3)	1.912(1)
V1–O4a	1.940(2)	1.933(1)	V1–O4b	1.928(2)	1.920(1)
V1–N2a	2.031(3)	2.032(1)	V1–N2b	2.043(3)	2.044(2)
O3a–V1–O4a	136.3(1)	136.59 (5)	O4a–V1–N2a	83.8(1)	83.73(5)
O3b–V1–O4b	135.5(1)	134.71(5)	O4b–V1–N2b	83.9(1)	83.74(6)
O3a–V1–O4b	86.1(1)	85.10(5)	O3a–V1–N2b	88.1(1)	87.71(5)
O3b–V1–O4a	84.7(1)	83.36(5)	O3b–V1–N2a	86.3(1)	87.81(5)
O4b–V1–N2a	133.0(1)	132.53(6)	N2a–V1–N2b	136.7(1)	136.38(6)
O4a–V1–N2b	131.1(1)	131.43(5)	O3b–V1–O3a	130.6(1)	131.86(5)
O3a···N2a	2.417(3)	2.415(3)	O3b···N2b	2.406(3)	2.395(4)
O4a···O4b	2.505(2)	2.531(2)			
O3a–V1–N2a	75.3(1)	74.92(5)	O3b–V1–N2b	74.6(1)	74.47(5)
O4a–V1–O4b	80.8(1)	82.21(5)			

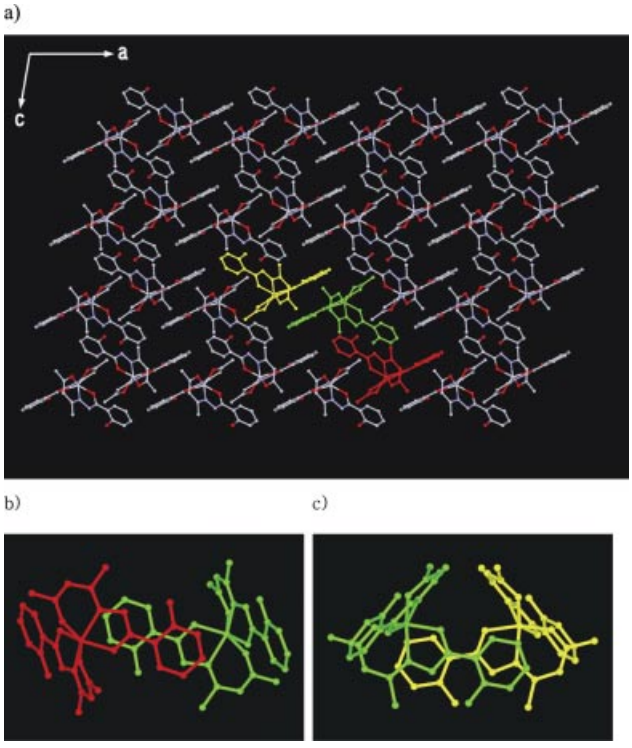

Figure 5. (a) Packing of **2a**. (b) Type-III π–π stacking interaction. (c) Type-IV π–π stacking interaction.

The same type III interaction is also observed in the packing of **2b** (Figure 6, b). However, the same π–π stacked dimeric species formed by the type III interaction is connected by a different type of π–π stacking interaction (type V) with the neighboring dimeric species to form a one-dimensional chain in **2b** (Figure 6, a and c).

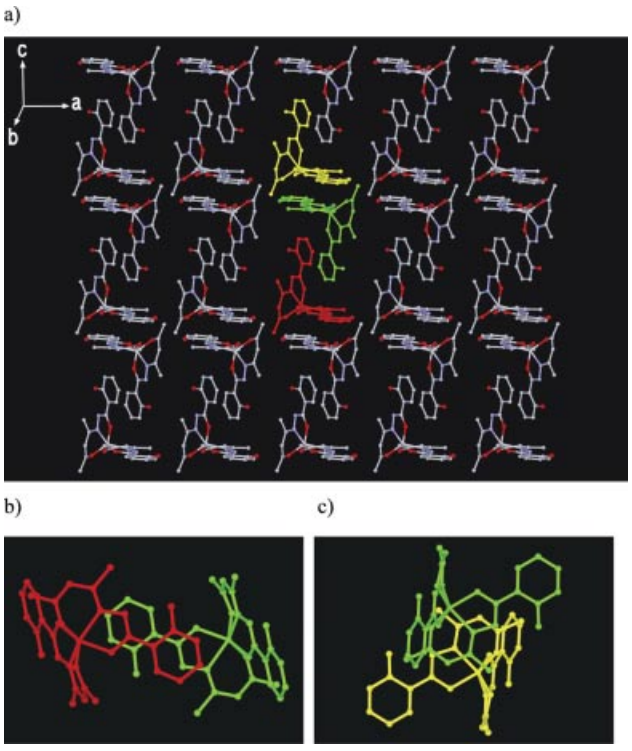

Figure 6. (a) Packing of **2b**. (b) Type-III π–π stacking interaction. (c) Type-V π–π stacking interaction.

Thermal Stability

The TGA and DSC data for polymorphic vanadium crystals **1a**, **1b**, **2a**, and **2b** were obtained in air. The data for **1a** indicate multistage weight loss with the related endotherms and exotherms (Figure 7, a). The first weight loss, related to the first endotherm near 106 °C, can be assigned as the loss of about one equivalent of water (found: 4.97%; calcd.: 4.95%). Even though no water molecules were observed in the crystal structure, water molecules in air are probably physisorbed on the surface of **1a**.[18] The second endotherm near 116 °C, with no weight loss, is assigned to the melting of **1a**. This assignment was also supported by the melting point measurement of a crystal of **1a**. Additional multistage weight loss was observed between 125 and 500 °C. At least four exotherms in the DSC could be related to weight loss in the TGA. However, the decomposition pattern of **1a** could not be followed in detail due to overlapping decomposition steps. The TGA and DSC data for **1b** also indicated multistage weight loss with related endotherms and exotherms (Figure 7, b). The first weight loss occurs near 108 °C and can also be assigned to the loss of about one equivalent of water (found: 5.03%; calcd.: 4.97%). The second endotherm near 118 °C is again assigned to the melting of crystal **1b**. Similar multi-step weight loss and related exotherms are observed to those in crystal **1a**. The thermal properties of the polymorphs are very similar to each other, but not identical. The melting point of crystal **1b** is slightly higher than that of crystal **1a**, even though only one type of π–π stacking interaction is observed in crystal **1b**, while a second type of π–π stacking interaction is also observed in crystal **1a**.

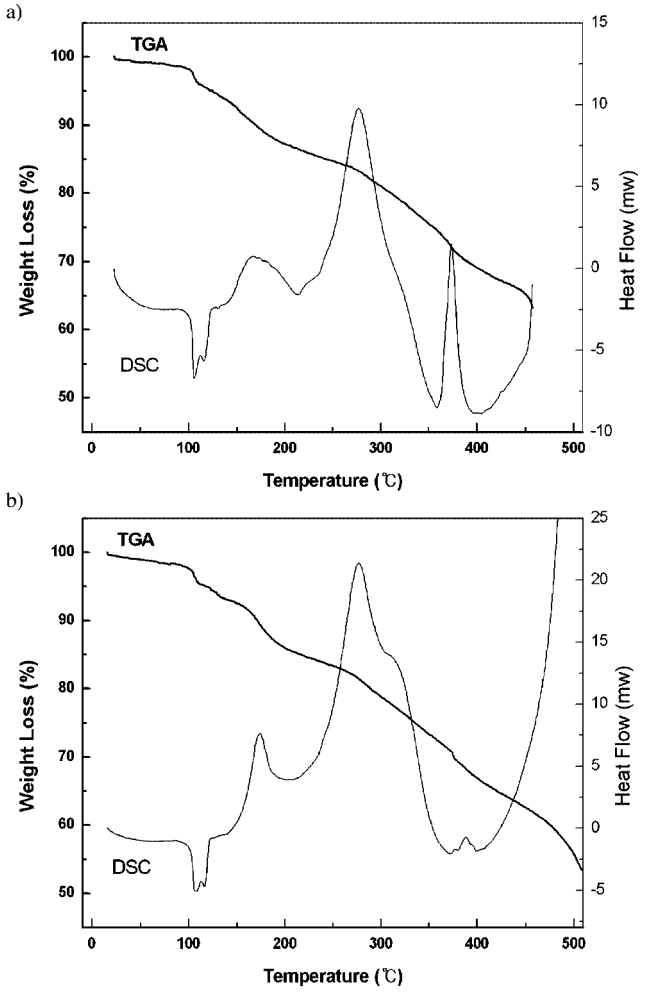

Figure 7. TGA and DSC curves for (a) crystals of **1a** and (b) crystals of **1b**.

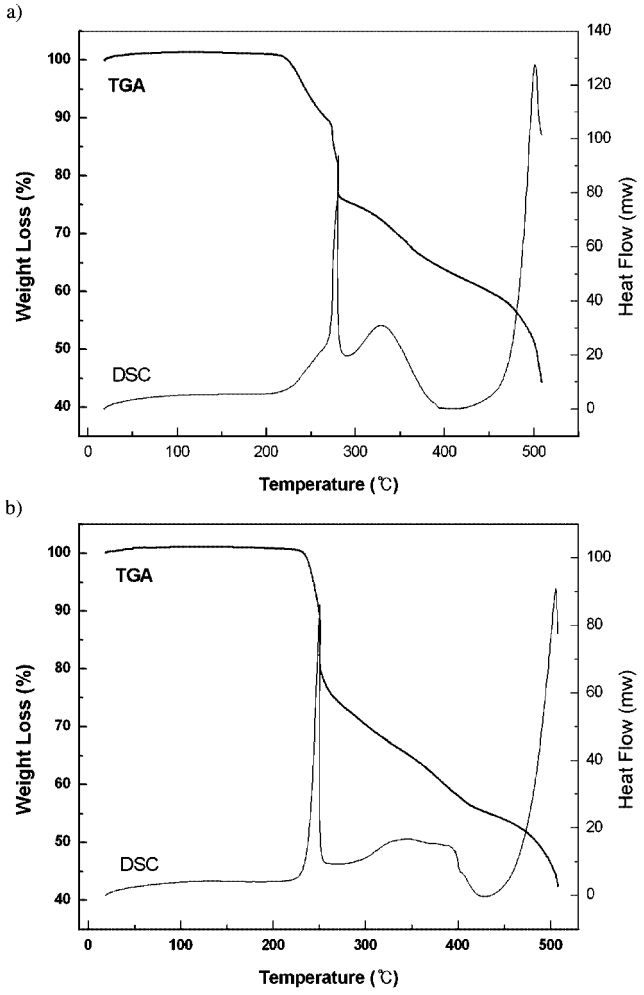

Figure 8. TGA and DSC curves for (a) crystals of **2a** and (b) crystals of **2b**.

The TGA and DSC data for **2a** and **2b** do not show any indication of weight loss or phase transition up to about 200 °C (Figure 8). Crystal **2a** starts an (at least) four-step weight loss around 220 °C (Figure 8, a). The TGA and DSC data for **2b** are also similar to those of crystal **2a**, but not identical (Figure 8, b). Crystal **2b** starts a fast weight loss around 230 °C. The TGA and DSC data for **2a** and **2b** imply that crystals of **2a** and **2b** have slightly different decomposition pathways. The decomposition pattern of crystals **2a** and **2b** could not be followed in detail due to overlapping decomposition steps.

Conclusions

We have prepared two polymorphs of vanadium(IV) and vanadium(V) complexes under slightly different conditions. Depending on the ratio of ligand to metal ion, various polymorphs can be obtained as both mixtures and pure crystal forms. We assume that the extent of exposure to oxygen also affects the formation of polymorphs. The amount of oxygen affects the amount of vanadium(IV) complex in solution, and the precipitation and filtration of the vanadium(IV) intermediate changes the composition of the related species in solution. The mononuclear mono-oxo mono-alkoxo square-pyramidal vanadium(V) complex [$V^{V}O$(Hacshz)(OEt)] (**1**), in two different polymorphs (**1a** and **1b**), was prepared by simple addition of one equivalent of vanadium(III) acetylacetonate to an ethanol solution of H_3shz. The same type of π–π stacking interaction mode (type I) is observed in both polymorphs. This interaction mode results in the very similar dimeric species observed in both polymorphs. While van der Waals interactions between the π–π stacked dimeric species result in polymorph **1b**, a combination of type II interactions and van der Waals interactions between the π–π stacked dimeric species results in polymorph **1a**.

The mononuclear vanadium(IV) complex [V^{IV}(Hacshz)$_2$] (**2**) was obtained as an intermediate or side product in the formation of complex **1** with limited amounts of oxygen, or was alternatively prepared with H_3shz and vanadyl(IV) acetylacetonate in methanol under nitrogen. As in complex **1**, the same (type III) interaction was observed in both polymorphs **2a** and **2b**. This interaction mode again results in the same dimeric species existing in both crystals. Two dif-

ferent types of π–π stacking interactions (type IV and type V) result in two polymorphs (**2a** and **2b**).

The prenucleation step involves the same dominant π–π stacking in solution, and two subsequent nearly isoenergetic packing modes may be the reason for the formation of the two polymorphs in both complexes **1** and **2**.

The thermal properties, such as the decomposition behavior and melting points, of the two different polymorphs of the same vanadium complexes are very similar, but not identical.

Experimental Section

Materials and Instrumentation: The following were used as received with no further purification: salicylhydrazide (H_3shz), vanadium(III) acetylacetonate, [D_6]dimethyl sulfoxide, and [D]chloroform from Aldrich, Inc.; ethanol (EtOH) from Carlo–Erba. The determination of C, H, and N contents was performed at the Elemental Analysis Laboratory of the Korean Institute of Basic Science, Seoul. Infrared spectra were recorded from KBr pellets in the spectral range 4000–600 cm^{-1} with a Bio-Rad FT-IR spectrophotometer. Absorption spectra were obtained with a Shimadzu UV-2401PC spectrophotometer. ^{1}H-NMR spectra were obtained with a Varian-300 spectrometer. Room-temperature magnetic susceptibilities of well-ground solid samples were measured using the Evans method.[15] Melting points of well-ground solid samples were measured with a Sanyo Gallenkamp PLC melting point apparatus. Thermogravimetric analysis (TGA) and differential scanning calorimetry (DSC) data were obtained simultaneously with a SCINCO STA S-1000.

Synthesis of [V^{V}O(Hacshz)(OEt)] (1): Complex **1** was synthesized following the reported method.[14] H_3shz (0.234 g, 1.53 mmol) was dissolved in 15 mL of ethanol in a 50-mL beaker. One equivalent of vanadium(III) acetylacetonate (0.531 g, 1.52 mmol) was then added to the solution, whereupon the solution changed color to dark brown. After 20 min of stirring, the solution was filtered. Slow evaporation of the filtrate in air over three days produced dark crystals (0.270 g, 51.4%). A mixture of two different colored crystals, with dark greenish-brown crystals as the major component and dark-reddish-brown crystals as the minor component, could be noticed upon careful visual examination. IR data for the mixture: $\tilde{\nu}$ = 1622, 1597, 1543, 1502, 1489, 1432, 1376, 1328, 1305, 1286, 1255, 1158, 1085, 1033, 1000, 954, 916, 825, 791, 761, 717, 696, 662, 600 cm^{-1}.

[V^{V}O(Hacshz)(OEt)] (1a). Method A: H_3shz (0.234 g, 1.53 mmol) was dissolved in 15 mL of ethanol in a 30-mL vial fitted with a cap. One equivalent of vanadium(III) acetylacetonate (0.531 g, 1.52 mmol) was then added to the solution, whereupon the solution changed color to dark brown. The solution was filtered after stirring for 5 min. Dark-bluish-brown crystals of [V^{IV}(Hacshz)$_2$] (**2**) formed from the solution over one day and were filtered off. Allowing the the filtrate to stand for a further three days in a vial gave dark-greenish-brown crystals of **1a**.

Method B: H_3shz (0.234 g, 1.53 mmol) was dissolved in 15 mL of ethanol in a 50-mL beaker. Half an equivalent of vanadium(III) acetylacetonate (0.262 g, 0.752 mmol) was added to the solution, whereupon the solution changed color to dark brown. The solution was filtered after stirring for 5 min. Slow evaporation of the filtrate in air gave dark-greenish-brown crystals of **1a** after three days (0.126 g, 48.6%). [V^{V}O(Hacshz)(OEt)]·H_2O ($C_{14}H_{19}N_2O_6V$; M = 362.26): calcd. C 46.42, H 5.29, N 7.73, V 14.06; found C 46.51, H 5.11, N 8.12, V 14.06. Selected IR bands (KBr): $\tilde{\nu}$ = 1622, 1598, 1545, 1491, 1431, 1385, 1349, 1307, 1288, 1256, 1160, 1086, 1041, 998, 953, 919, 826, 788, 758, 713, 696, 659, 606 cm^{-1}. M.p. 115.1–116.9 °C.

[V^{V}O(Hacshz)(OEt)] (1b): H_3shz (0.234 g, 1.53 mmol) was dissolved in 15 mL of ethanol in a 50-mL beaker. One-third of an equivalent of vanadium(III) acetylacetonate (0.174 g, 0.500 mmol) was then added to the solution, whereupon the solution changed color to dark brown. The solution was filtered after stirring for 5 min. Slow evaporation of the filtrate in air gave dark-reddish-brown crystals of **1b** after four days (0.0554 g, 32.2%). [V^{V}O(Hacshz)(OEt)]·H_2O ($C_{14}H_{19}N_2O_6V$; M = 362.26): calcd. C 46.42, H 5.29, N 7.73, V 14.06; found C 46.74, H 4.98, N 8.14, V 14.50. Selected IR bands (KBr): $\tilde{\nu}$ = 1619, 1599, 1546, 1503, 1490, 1432, 1382, 1346, 1304, 1286, 1254, 1159, 1085, 1035, 1001, 954, 916, 824, 789, 760, 718, 694, 660, 599 cm^{-1}. M.p. 117.2–118.8 °C.

[V^{IV}(Hacshz)$_2$] (2): Two different shaped dark crystals were observed in the precipitate (0.254 g, 32.9%) obtained during the synthesis of **1a** using method A. Most of them were block-shaped, dark-bluish-brown crystals of **2a**, while a few crystals with a different morphology (**2b**) were also noticed. Elemental analysis and spectroscopic analysis were performed with **2a**. V^{IV}(Hacshz)$_2$ ($C_{24}H_{24}N_4O_6V$; M = 515.42): calcd. C 55.93, H 4.69, N 10.87, V 9.88; found C 55.77, H 4.66, N 10.54, V 9.93. Selected IR bands (KBr): $\tilde{\nu}$ = 1623, 1589, 1536, 1485, 1464, 1421, 1375, 1320, 1256, 1159, 1112, 1032, 960, 946, 878, 858, 826, 795, 772, 761, 752, 716, 697, 663, 599 cm^{-1}. Decomposition temperature: 212.6–214.2 °C. μ_{eff} = 1.80 μ_B.

[V^{IV}(Hacshz)$_2$] (2b): Compound **2b** was synthesized following a reported method.[16] H_3shz (0.761 g, 5.0 mmol) was dissolved in 40 mL of anhydrous methanol in a 100-mL round-bottomed flask. Half an equivalent of vanadyl(IV) acetylacetonate (0.663 g, 2.50 mmol) was then added to the solution, whereupon the solution changed color to dark brown. After 40 min of refluxing under nitrogen, the solution was cooled. The deep-purple precipitate formed was filtered off and washed with methanol and hexane (0.661 g, 51.3%). V^{IV}(Hacshz)$_2$ ($C_{24}H_{24}N_4O_6V$; M = 515.42): calcd. C 55.93, H 4.69, N 10.87, V 9.88; found C 55.77, H 4.66, N 10.54, V 11.00. Selected IR bands (KBr): $\tilde{\nu}$ = 1624, 1588, 1536, 1485, 1419, 1376, 1328, 1319, 1256, 1158, 1111, 1091, 1032, 1023, 1013, 961, 945, 878, 858, 825, 794, 772, 762, 752, 717, 705, 696, 663, 599 cm^{-1}. Decomposition temperature: 216.8–217.6 °C.

X-ray Crystallography: Crystals of complexes **1a**, **1b**, **2a**, and **2b** were mounted on a glass fiber. Preliminary examination and data collection were performed using a Bruker SMART CCD Detector single-crystal X-ray diffractometer equipped with a graphite-monochromated Mo-K_α radiation source (λ = 0.71073 Å) equipped with a sealed tube X-ray source operating at –100 °C. Preliminary unit-cell constants were determined from a set of 45 narrow frame scans (0.3° in ω). The data sets collected consisted of 1286 frames of intensity data, collected using a frame width of 0.3° in ω, and a count time of 10 seconds per frame, with a crystal-to-detector distance of 5 cm. The double pass scanning method was used to exclude any noise. The collected frames were integrated using an orientation matrix determined from the narrow frame scans. The SMART and SAINT software packages[19] were used for data collection and integration, respectively. Analysis of the integrated data did not show any decay. The final cell constants were determined using a global refinement of 8192 reflections ($\theta < 25.0°$). Collected data were corrected for absorbance using the SADABS package[20] based upon the Laue symmetry using equivalent reflections. The structural solution and refinement of the structure were carried out

Table 4. Crystal data and structure refinement for **1**, **1b**, **2a**, and **2b**.

	1a	**1b**	**2a**	**2b**
Formula	$C_{14}H_{17}N_2O_5V$	$C_{14}H_{17}N_2O_5V$	$C_{24}H_{24}N_4O_6V$	$C_{24}H_{24}N_4O_6V$
Formula weight	344.24	344.24	515.41	515.41
Crystal system	monoclinic	triclinic	monoclinic	triclinic
Space group	$P2_1/c$	$P\bar{1}$	$C2/c$	$P\bar{1}$
a [Å]	10.3275(7)	7.0798(6)	27.083(5)	9.7242(9)
b [Å]	14.838(1)	10.3111(9)	9.929(2)	10.1706(9)
c [Å]	10.7251(8)	11.028(1)	18.033(3)	13.547(1)
α [°]	90	80.415(2)	90	100.602(2)
β [°]	113.864(1)	88.745(2)	99.673(3)	94.152(2)
γ [°]	90	71.767(1)	90	112.984 (1)
V [Å^3]	1503.0(2)	753.6(1)	4780(2)	1196.9(2)
Z	4	2	8	2
Crystal size [mm]	0.32×0.25×0.20	0.70×0.45×0.18	0.30×0.13×0.10	0.45×0.35×0.25
θ range [°]	2.16–28.31	2.11–28.26	1.53–28.29	2.24–28.28
GOF on F^2	1.072	1.090	1.021	1.055
Final R [$I > 2\sigma(I)$]	$R1$[a] = 0.0310 $wR2$[b] = 0.0837	$R1$ = 0.0274 $wR2$ = 0.0766	$R1$ = 0.0698 $wR2$ = 0.1199	$R1$ = 0.0357 $wR2$ = 0.0927
R (all data)	$R1$ = 0.0364 $wR2$ = 0.0875	$R1$ = 0.0287 $wR2$ = 0.0775	$R1$ = 0.1393 $wR2$ = 0.1397	$R1$ = 0.0452 $wR2$ = 0.0986
Largest diff. peak and hole [e Å^{-3}]	0.411 & –0.198	0.304 & –0.339	0.614 & –0.311	0.451 & –0.228

[a] $R1 = \Sigma||F_o| - |F_c||/\Sigma|F_o|$. [b] $wR2 = [\Sigma w(F_o^2 - F_c^2)^2/\Sigma wF_o^4]^{1/2}$.

using the SHELXTL v5.1 software package.[21] All non-hydrogen atoms were refined anisotropically. In **1a**, hydrogen atoms were refined isotropically, except for the hydrogen atoms of the disordered ethoxide, which were refined with assigned isotropic displacement coefficients U(H) = 1.2 U(C) or 1.5 $U(C_{methyl})$ on their respective atoms. In **1b** and **2b**, all hydrogen atoms were refined isotropically. In **2a**, hydrogen atoms were refined with assigned isotropic displacement coefficients U(H) = 1.2 U(C) or 1.5 $U(C_{methyl})$ on their respective atoms, except for two phenolic hydrogen atoms, which were refined isotropically. The crystal and intensity data are shown in Table 4.

CCDC-262588 to -262591 contain the supplementary crystallographic data for this paper. These data can be obtained free of charge from The Cambridge Crystallographic Data Centre via www.ccdc.cam.ac.uk/data_request/cif.

Acknowledgments

We thank the Korean Institute of Basic Science for performing the elemental analyses. The authors wish to acknowledge the financial support of the Korea Research Foundation (grant KRF-2002-070-C00053), KISTEP (M1-0213-03-0004), and CBMH.

[1] a) D. Braga, F. Grepioni, G. R. Desiraju, *Chem. Rev.* **1998**, *98*, 1375; b) J. C. M. Rivas, L. Brammer, *Coord. Chem. Rev.* **1999**, *183*, 43; c) D. C. Sherrington, K. A. Taskinen, *Chem. Soc. Rev.* **2001**, *30*, 83; d) M. Yamanaka, A. Shivanyuk, J. Rebek, *J. Am. Chem. Soc.* **2004**, *126*, 2939; e) R. H. Vreekamp, J. P. M. Van Duynhoven, M. Hubert, W. Verboom, D. N. Reinhoudt, *Angew. Chem. Int. Ed. Engl.* **1996**, *35*, 1215.

[2] a) G. Forster, A. Meister, A. Blume, *Phys. Chem. Chem. Phys.* **2000**, *2*, 4503; b) N. Vembu, M. Nallu, S. Durmus, M. Pazner, J. Garrison, W. J. Youngs, *Acta Crystallogr., Sect. C* **2004**, *60*, o65–o68.

[3] a) S. Lee, A. B. Mallik, D. C. Fredrickson, *Cryst. Growth Des.* **2004**, *4*, 279; b) S. P. Anthony, T. P. Radhakrishnan, *Chem. Commun.* **2001**, 931.

[4] a) C. A. Hunter, J. K. M. Sanders, *J. Am. Chem. Soc.* **1990**, *112*, 5525; b) P. J. Nichols, C. L. Raston, J. W. Steed, *Chem. Commun.* **2001**, 1062; c) P. L. Caradoc-Davies, L. R. Hanton, *Chem. Commun.* **2001**, 1098; d) A. Magistrato, P. S. Pregosin, A. Albinati, U. Rothlisberger, *Organometallics* **2001**, *20*, 4178.

[5] a) B. J. Holliday, C. A. Mirkin, *Angew. Chem. Int. Ed.* **2001**, *40*, 2022; b) M. Fujita, *Chem. Soc. Rev.* **1998**, *27*, 417; c) B. Olenyuk, J. A. Whiteford, A. Fechtenkotter, P. J. Stang, *Nature* **1999**, *398*, 796; d) A. B. Mallik, S. Lee, E. B. Lobkovsky, *Cryst. Growth Des.* **2005**, *ASAP*; e) B. Chen, S. Lee, D. Venkataraman, F. J. DiSalvo, E. Lobkovsky, M. Nakayama, *Cryst. Growth Des.* **2002**, *2*, 101; f) O. R. Evans, W. Lin, *Chem. Mater.* **2001**, *13*, 2705.

[6] a) A. Ajayaghosh, S. J. George, *J. Am. Chem. Soc.* **2001**, *123*, 5148; b) P. Gamez, G. A. van Albada, I. Mutikainen, U. Turpeinen, J. Reedijk, *Inorg. Chim. Acta* **2005**, *358*, 1975; c) A. M. Plokhotnichenko, E. D. Radchenko, S. G. Stepanian, L. Adamovicz, *J. Phys. Chem.* **1999**, *103*, 11052; d) D. Braga, L. Maini, L. Prodi, A. Caneschi, R. Sessoli, F. Grepioni, *Chem. Eur. J.* **2000**, *6*, 1310; e) Y. Wang, R. Cao, W. Bi, X. Li, D. Sun, *J. Mol. Struct.* **2005**, *738*, 53; f) D. Braga, L. Maini, M. Polito, M. Rossini, F. Grepioni, *Chem. Eur. J.* **2000**, *6*, 4227; g) Y. Kim, J. G. Verkade, *Inorg. Chem.* **2003**, *42*, 4262; h) A. Y. Ziganshina, Y. H. Ko, W. S. Jeon, K. Kim, *Chem. Commun.* **2004**, 806–807; i) M. Oh, G. B. Carpenter, D. A. Sweigart, *Chem. Commun.* **2002**, 2168; j) W. Lu, M. C. W. Chan, K. Cheung, C. Che, *Organometallics* **2001**, *20*, 2477; k) D. D. Graf, R. G. Duan, J. P. Campbell, L. L. Miller, K. R. Mann, *J. Am. Chem. Soc.* **1997**, *119*, 5888.

[7] a) A. B. Mallik, S. Lee, L. Tran, E. B. Lobkovsky, *Cryst. Growth Des.* **2003**, *3*, 467; b) W. A. Herrebout, T. V. D. Kerkhof, B. J. van der Veken, *Phys. Chem. Chem. Phys.* **2000**, *2*, 4925; c) R. Ricceri, N. V. Romeu, G. Taddei, *Langmuir* **1996**, *12*, 913; d) E. S. Lee, K. Na, Y. H. Bae, *Nano Lett.* **2005**, *ASAP*; e) M. Oishi, Y. Nagasaki, K. Itaka, N. Nishiyama, K. Kataoka, *J. Am. Chem. Soc.* **2005**, *127*, 1624; f) A. Rösler, G. W. M. Vandermeulen, H. Klok, *Adv. Drug Delivery Rev.* **2001**, *53*, 95.

[8] a) F. H. Herbstein, *Cryst. Growth Des.* **2004**, *4*, 1419; b) J. Bernstein, R. J. Davey, J. O. Henck, *Angew. Chem. Int. Ed.* **1999**, *38*, 3440; c) D. Braga, L. Maini, M. Polito, L. Scaccianoce, G. Cojazzi, F. Grepioni, *Coord. Chem. Rev.* **2001**, *216–217*, 225; d) T. Kawamura, Y. Miyazaki, M. Sorai, *Chem. Phys. Lett.* **1997**, *273*, 435; e) A. Kalman, L. Fabian, G. Argay, G. Bernath, Z. Gyarmati, *J. Am. Chem. Soc.* **2003**, *125*, 34.

[9] a) A. Matsumoto, T. Tanaka, T. Tsubouchi, K. Tashiro, S. Saragai, S. Nakamoto, *J. Am. Chem. Soc.* **2002**, *124*, 8891; b) J. A. McMahon, M. J. Zaworotko, J. F. Remenar, *Chem. Commun.* **2004**, 278; c) V. R. Thalladi, M. Nüsse, R. Boese, *J. Am. Chem. Soc.* **2000**, *122*, 9227; d) J. M. Barendt, E. G. Bent, R. C. Haltiwanger, C. A. Squier, A. D. Norman, *Inorg. Chem.* **1989**, *28*, 4425.
[10] a) D. L. Reger, J. R. Gardinier, M. D. Smith, A. M. Shahin, G. J. Long, L. Rebbouh, F. Grandjean, *Inorg. Chem.* **2005**, *44*, 1852; b) H. Birkedal, H. B. Burgi, K. Komatsu, D. Schwarzenbach, *J. Mol. Struct.* **2003**, *647*, 233; c) S. M. Reed, T. J. R. Weakley, J. E. Hutchison, *Cryst. Eng.* **2000**, *3*, 85; d) L. Ballester, A. M. Gil, A. Gutiérrez, M. F. Perpinan, M. T. Azcondo, A. E. Sanchez, U. Amador, J. Campo, F. Palacio, *Inorg. Chem.* **1997**, *36*, 5291.
[11] a) R. Kato, *Chem. Rev.* **2004**, *104*, 5319; b) R. P. Shibaeva, E. B. Yagubskii, *Chem. Rev.* **2004**, *104*, 5347; c) T. Inabe, H. Tajima, *Chem. Rev.* **2004**, *104*, 5503.
[12] a) H. Tseng, S. A. Vignon, J. F. Stoddart, *Angew. Chem. Int. Ed.* **2003**, *42*, 1491; b) W. S. Jeon, A. Y. Ziganshina, J. W. Lee, Y. H. Ko, J. Kang, C. Lee, K. Kim, *Angew. Chem. Int. Ed.* **2003**, *42*, 4097.
[13] a) C. P. Collier, E. W. Wong, M. Belohradsky, F. M. Raymo, J. F. Stoddart, P. J. Kuekes, R. S. Williams, J. R. Heath, *Science* **1999**, *285*, 391; b) L. Fu, L. Cao, Y. Liu, D. Zhu, *Adv. Colloid Interface Sci.* **2004**, *111*, 133; c) J. R. Reimers, A. Bilic, Z. Cai, M. Dahlbom, N. A. Lambropoulos, G. C. Solomon, M. J. Crossley, N. S. Hush, *Aust. J. Chem.* **2004**, *57*, 1133.
[14] M. Moon, M. Pyo, Y. C. Myoung, C. I. Ahn, M. S. Lah, *Inorg. Chem.* **2001**, *40*, 554–557.
[15] D. F. Evans, *J. Chem. Soc.* **1958**, 2003.
[16] A. A. Dianantis, M. Manikas, M. A. Salam, M. R. Snow, E. R. T. Tiekink, *Aust. J. Chem.* **1988**, *41*, 453–468.
[17] The twist angles were calculated by taking the average of the angles made by the projection of the vertices of the top and bottom faces along the direction of the two centroids of the trigonal faces.
[18] The elemental analysis data are also in conformity with TGA results.
[19] *SMART* and *SAINT*, Area Detector Software Package and SAX Area Detector Integration Program; Bruker Analytical X-ray; Madison, WI, USA, **1997**.
[20] *SADABS*, Area Detector Absorption Correction Program; Bruker Analytical X-ray, Madison, WI, USA, **1997**.
[21] G. M. Sheldrick, *SHELXTL-PLUS*, Crystal Structure Analysis Package; Bruker Analytical X-ray; Madison, WI, USA, **1997**.

Received: March 16, 2005
Published Online: November 2, 2005

